COMPDYN 2011
3^{rd} ECCOMAS Thematic Conference on
Computational Methods in Structural Dynamics and Earthquake Engineering
M. Papadrakakis, M. Fragiadakis, V. Plevris (eds.)
Corfu, Greece, 25-28 May 2011

HYBRID LAPLACE-TIME DOMAIN APPROACH FOR NONLINEAR DYNAMIC SOIL-STRUCTURE INTERACTION PROBLEMS

A. Nieto Ferro[1,2], D. Clouteau[1], N. Greffet[2] and G. Devésa[2]

[1]LMSSMat (CNRS UMR 8579) - Ecole Centrale Paris
Grande Voie des Vignes, 92295 Châtenay-Malabry, France
e-mail: {didier.clouteau,alex.nieto-ferro}@ecp.fr

[2]Electricité de France R&D - Dept. AMA
Avenue du Général de Gaulle 1, 92141 Clamart, France
e-mail: {nicolas.greffet, georges.devesa}@edf.fr

Keywords: Dynamic soil-structure interaction, impedance matrix, hybrid Laplace-time domain approach, Convolution Quadrature Method, nonlinear analysis.

Abstract. *Nonlinear dynamic soil-structure interaction problems are usually solved by a substructuring technique where the soil-structure system is decomposed into two sub-domains: the nonlinear structure, which can also include a part of the soil showing a nonlinear behavior, and the linear unbounded soil. The present work considers the case where the problem is localized on the building. The effects of the unbounded soil are then represented as a particular type of boundary condition by means of the so-called impedance operator, assumed to be known in the Laplace domain. In this framework, since nonlinearities are taken into account, the problem has to be solved in the time domain. Consequently, the interaction forces are expressed in terms of the Laplace-domain impedance results as a convolution integral between the time impedance coefficients and the nodal displacements located on the interface. In order to compute this convolution product a hybrid Laplace-time domain approach based on a Convolution Quadrature Method is introduced. It allows to express this convolution not only in terms of displacements but also in terms of accelerations and velocities convolutions. The proposed method is finally tested on a soil-structure application modeled with a lumped-parameter system. Satisfactory results are obtained when an elasto-plastic behaviour is accounted for.*

1 INTRODUCTION

The classical dynamic soil-structure interaction method is based on a domain decomposition technique, where the whole soil-structure domain is decomposed into two subdomains: the soil and the structure. Both subdomains lead to a local problem that is solved separately, warranting in a conformal approach that the traction equilibrium and displacement continuity are verified on the soil-structure interface. The main reason for this decomposition is that different numerical methods can be used for the soil and for the structure. On the one hand, the bounded subdomain of the structure can be modeled by means of a Finite Element method which allows to take into account nonlinear phenomena in a straightforward way. On the other, the unbounded linear elastic soil can be computed using a Boundary Element method, the radiation conditions being thus implicitly satisfied. When the soil shows a nonlinear behaviour, the corresponding part of this subdomain should be incorporated to the structure subdomain.

Since engineers are usually more interested in the structural response, the global problem is solved directly in the building and the effect of the soil is taken into account as a particular type of boundary condition. This condition is expressed by means of the so-called impedance operator which, in the present work, is assumed to be known in the Laplace domain. The matrix impedance $s \mapsto \hat{\boldsymbol{Z}}(\boldsymbol{s}), s \in \mathbb{C}$, i.e. the discretized version of the impedance operator, maps any displacement vector of the soil-structure interface to its corresponding force vector on the same boundary.

When nonlinearities are accounted for, the problem have to be formulated in the time domain. Consequently, the interaction forces on the soil-structure interface denoted by Γ result in a convolution product between the time dynamic impedance coefficients $t \mapsto \boldsymbol{Z}(t)$ and the degrees-of-freedom of the nodes located on the interface $t \mapsto \boldsymbol{u}_\Gamma(t), t \in \mathbb{R}$:

$$(\boldsymbol{Z} * \boldsymbol{u}_\Gamma)(t) = \int_0^t \boldsymbol{Z}(t-\tau)\boldsymbol{u}_\Gamma(\tau)\, d\tau, \quad 0 \leq t \leq T \tag{1}$$

where the impedance is assumed to satisfy causality properties.

In order to compute this kind of convolution integrals, literature proposes different numerical methods, such as the frequency-time method [1, 2] or the hidden variables method [3], which are based on a frequency domain formulation of the impedance operator. Similarly, some authors have focused on formulations in the Laplace domain [4, 5], showing a special interest when coupled to a Convolution Quadrature Method (CQM) [6].

The approach presented in this article is in essence an extension of the work originally proposed by Moser and al. [7, 8] and Pereira and Beer [9]. A hybrid Laplace-time domain technique is therefore introduced in the following sections in order to numerically evaluate Equation 1. Time is discretized by means of a CQM, so the Laplace transform of the convolution kernel is supposed to be analytic on the complex half-plane $\Re e(s) > \sigma_0$ and polynomially bounded for large $|s|$:

$$||\hat{\boldsymbol{Z}}(s)|| \leq D|s|^\mu \tag{2}$$

for $D, \mu \in \mathbb{R}$. Particularly, the dynamic impedance matrix will be assumed of the following form:

$$\hat{\boldsymbol{Z}}(s) = \boldsymbol{M}_\Gamma s^2 + \boldsymbol{C}_\Gamma s + \boldsymbol{K}_\Gamma + \hat{\boldsymbol{Z}}_{ns}(s) \tag{3}$$

where $\boldsymbol{K}_\Gamma$,$\boldsymbol{C}_\Gamma$ and $\boldsymbol{M}_\Gamma$ are the matrices which correspond to the inertial, damping and stiffness effects and where $\hat{\boldsymbol{Z}}_{ns}(s)$ denotes a non-singular function vanishing for large $|s|$.

2 HYBRID LAPLACE-TIME DOMAIN APPROACH

In this framework, the CQM approximates the convolution integral in Equation 1 by a discrete convolution (time step $\Delta t > 0$):

$$(\boldsymbol{Z} * \boldsymbol{u})(n\Delta t) = \sum_{0 \leq n\Delta t \leq t} \boldsymbol{\Phi_k} \boldsymbol{u}(t - n\Delta t) \ , \quad t = \Delta t, 2\Delta t, 3\Delta t, ... \tag{4}$$

where coefficients $\boldsymbol{\Phi_k}$ correspond to the weights of the generating power series:

$$\sum_{k=0}^{+\infty} \Phi_k \zeta^k = \hat{\boldsymbol{Z}}\left(s_{\Delta t}\right) \tag{5}$$

The complex sampled values $s_{\Delta t}$ of the dynamic soil impedance are given by a rational function of a linear multistep method of order p satisfying strong A-stability conditions. For instance, let $s_{\Delta t}$ be $\frac{\delta(\zeta)}{\Delta t}$ where $\delta(\zeta)$ is the backward differentiation formula of $p = 2$ reading $\delta(\zeta) = \frac{3}{2} - 2\zeta + \frac{1}{2}\zeta^2$.

Nevertheless, paying attention to the physical units of Equation 1, it seems natural to express the convolution not only in terms of displacements, but also in terms of accelerations and velocities. To that end, the polynomial part $\hat{\boldsymbol{P}}(s)$ of the impedance is factorized yielding to:

$$\hat{\boldsymbol{Z}}(s) = \hat{\boldsymbol{Z}}_m(s)\hat{\boldsymbol{P}}(s) = \hat{\boldsymbol{Z}}_m(s)\left(\tilde{\boldsymbol{M}}_\Gamma s^2 + \tilde{\boldsymbol{C}}_\Gamma s + \tilde{\boldsymbol{K}}_\Gamma\right) \tag{6}$$

where $\tilde{\boldsymbol{K}}_\Gamma$, $\tilde{\boldsymbol{C}}_\Gamma$ and $\tilde{\boldsymbol{M}}_\Gamma$ are respectively the estimators of the matrices $\boldsymbol{K}_\Gamma$,$\boldsymbol{C}_\Gamma$ and $\boldsymbol{M}_\Gamma$ presented in Equation 3.

Therefore, the convolution can be written in terms of the Laplace transform as follows:

$$(\boldsymbol{Z} * \boldsymbol{u})(t) = \frac{1}{2\pi i} \int_{\sigma_0 + i\mathbb{R}} \hat{\boldsymbol{Z}}_m(s)\hat{\boldsymbol{P}}(s)\hat{\boldsymbol{u}}(s)\, e^{st} ds \tag{7}$$

The polynomial function $\hat{\boldsymbol{P}}(s)$ acts thus over the displacement as a differential operator and Equation 1 finally reads:

$$(\boldsymbol{Z} * \boldsymbol{u})(t) = (\boldsymbol{Z}_m * \tilde{\boldsymbol{M}}_\Gamma \ddot{\boldsymbol{u}})(t) + (\boldsymbol{Z}_m * \tilde{\boldsymbol{C}}_\Gamma \dot{\boldsymbol{u}})(t) + (\boldsymbol{Z}_m * \tilde{\boldsymbol{K}}_\Gamma \boldsymbol{u})(t) \tag{8}$$

where the interaction force vector (denoted hereafter by $\boldsymbol{R}_\Gamma(t)$) involves in its calculation the evaluation of displacement, velocity and acceleration convolutions.

If a time step $\Delta t > 0$ is chosen, the convolution integral can be discretized again as in Equation 4 leading to:

$$\boldsymbol{R}_{\Gamma,n} = (\boldsymbol{Z} * \boldsymbol{u})(n\Delta t) = \sum_{k=1}^{n} \left(\boldsymbol{\Psi}_2^{n-k+1}\ddot{\boldsymbol{u}}_k + \boldsymbol{\Psi}_1^{n-k+1}\dot{\boldsymbol{u}}_k + \boldsymbol{\Psi}_0^{n-k+1}\boldsymbol{u}_k\right) \tag{9}$$

where matrices multiplying displacement vectors $\boldsymbol{u}_k$, velocity vectors $\dot{\boldsymbol{u}}_k$ and acceleration vectors $\ddot{\boldsymbol{u}}_k$ are given by:

$$\begin{aligned} \boldsymbol{\Psi}_0^k &= \boldsymbol{Z}_m^k \tilde{\boldsymbol{K}}_\Gamma \\ \boldsymbol{\Psi}_1^k &= \boldsymbol{Z}_m^k \tilde{\boldsymbol{C}}_\Gamma \\ \boldsymbol{\Psi}_2^k &= \boldsymbol{Z}_m^k \tilde{\boldsymbol{M}}_\Gamma \end{aligned} \tag{10}$$

From a numerical point of view, *sub-convolutions* are just unknown at $t = n\Delta t$, since all previous time steps have already been computed. Therefore, Equation 9 can be written by isolating instant n as:

$$\boldsymbol{R}_{\Gamma,n} = \boldsymbol{\Psi}_2^1 \ddot{\boldsymbol{u}}_n + \boldsymbol{\Psi}_1^1 \dot{\boldsymbol{u}}_n + \boldsymbol{\Psi}_0^1 \boldsymbol{u}_n + \boldsymbol{R}_{\Sigma(n-1)} \tag{11}$$

Consequently, coefficients $\boldsymbol{\Psi}_i^1 (i = 0, 1, 2)$ are respectively related to instantaneous stiffness, damping and inertia terms and $\boldsymbol{R}_{\Sigma(n-1)}$ depends only on previous time steps:

$$\boldsymbol{R}_{\Sigma(n-1)} = \sum_{k=1}^{n-1} \left(\boldsymbol{\Psi}_2^{n-k+1} \ddot{\boldsymbol{u}}_k + \boldsymbol{\Psi}_1^{n-k+1} \dot{\boldsymbol{u}}_k + \boldsymbol{\Psi}_0^{n-k+1} \boldsymbol{u}_k \right) \tag{12}$$

3 NUMERICAL APPLICATION

A lumped-parameter model is considered in the following in order to represent the soil-structure system. The nonlinear behaviour is introduced by an elastoplastic spring with one end attached to the upper mass m_1 and the other, to the smaller mass m_2. A square surface foundation layering on a homogeneous half-space is connected to mass m_2 by means of a rigid body constraint (see Figure 1). The soil impedance seen from the foundation is then computed with a boundary element method in the Laplace domain. For the sake of simplicity, the foundation is modeled to give an impedance in the form of inertial, damping and stiffness terms so that a time reference solution can be straightforwardly obtained. In order to illustrate some properties of the soil-structure system considered in an elastic regime, Table 1 gives the main eigenfrequencies of the structure clamped at its base.

	Pumping	Shaking	Torsional	Rocking
Eigenfrequencies [Hz]	5.43	7.95	99.86	405.34

Table 1: Main eigenfrequencies of the structure clamped at its base.

The soil can be characterized by its shear velocity $C_s = 505 m.s^{-1}$ and the elastoplastic behaviour of the spring is modeled with the linear kinematic work hardening law sketched in Figure 1. The elastic deformation is characterized here by the elastic stiffness matrix $\boldsymbol{K}_e$ which, after reaching the yield of plasticity $\boldsymbol{F}_y$, becomes $\boldsymbol{K}_p = 0.1\boldsymbol{K}_e$.

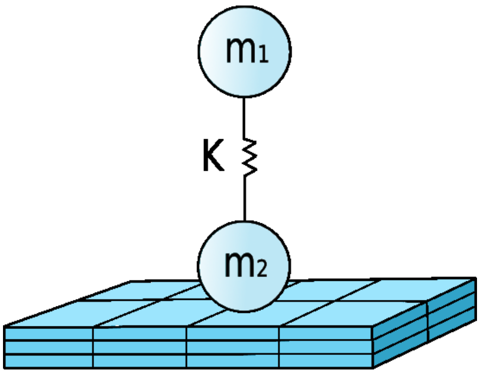

(a)

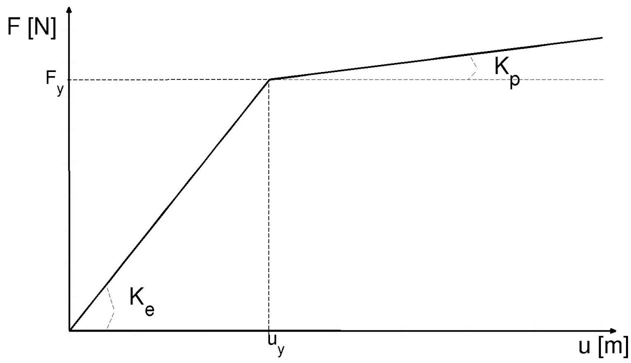

(b)

Figure 1: (a) Simplified model of a structure on a square surface foundation. (b) Linear kinematic work hardening law of the nonlinear spring K.

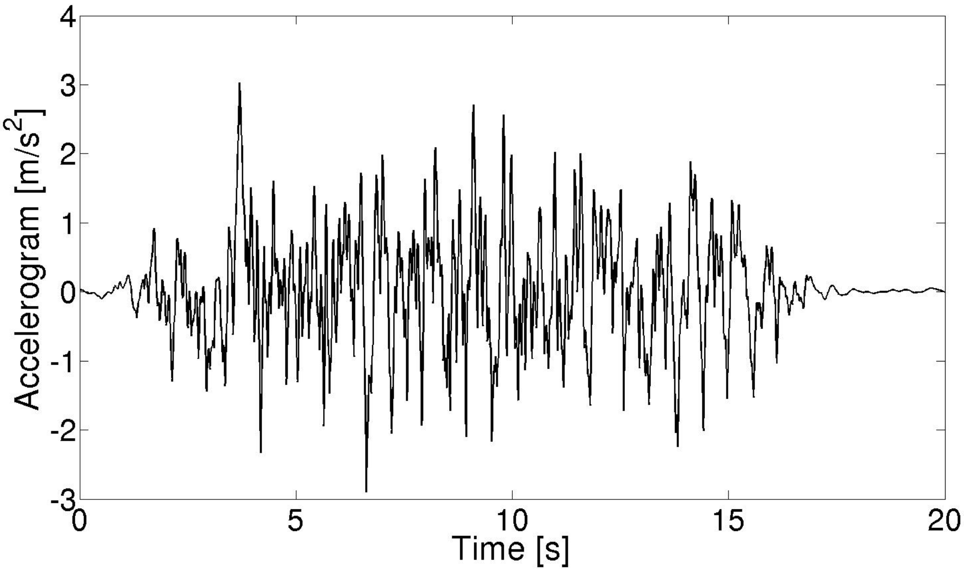

Figure 2: Free-field accelerogram applied to m_2 as a representation of the seismic loading.

The loading applied to m_2 in the x-direction $\boldsymbol{e}_x$ corresponds to the earthquake giving the free-field accelerogram $\gamma(t)$ shown in Figure 2, whose maximal acceleration is around $0.3g$.

The governing equations of this numerical model from the non-inertial frame of reference of the structure can be written at $t = n\Delta t$ as follows:

$$\begin{bmatrix} \boldsymbol{M}_{11} & \boldsymbol{0} \\ \boldsymbol{0} & \boldsymbol{M}_{22} + \boldsymbol{\Psi}_2^1 \end{bmatrix} \begin{bmatrix} \ddot{\boldsymbol{u}}_{1,n} \\ \ddot{\boldsymbol{u}}_{2,n} \end{bmatrix} + \begin{bmatrix} \boldsymbol{F}_{1,n}^{int} \\ \boldsymbol{F}_{2,n}^{int} \end{bmatrix} = \begin{bmatrix} -\boldsymbol{M}_1 \boldsymbol{e}_x \gamma_n \\ -\boldsymbol{M}_2 \boldsymbol{e}_x \gamma_n \end{bmatrix} + \begin{bmatrix} \boldsymbol{0} \\ -\boldsymbol{R}_{\Sigma(n-1)} \end{bmatrix} \tag{13}$$

where $\boldsymbol{F}_\alpha^{int}(t)$ ($\alpha \in \{1, 2\}$) denote the nonlinear internal efforts in the structure and depend on both displacement and velocity vectors. The interaction forces $\boldsymbol{R}_{\Gamma,n}$ have been directly substituted by Equation 11. It has to be noticed that the application considered here is particularized to the case where $\tilde{\boldsymbol{K}}_\Gamma = \tilde{\boldsymbol{C}}_\Gamma = \boldsymbol{0}$, that is the case where only inertial terms are taken into account for the computation of the convolution integral:

$$\boldsymbol{R}_{\Gamma,n} = \sum_{k=1}^{n} \boldsymbol{\Psi}_2^{n-k+1} \ddot{\boldsymbol{u}}_{2,k} = \boldsymbol{\Psi}_2^1 \ddot{\boldsymbol{u}}_{2,n} + \sum_{k=1}^{n-1} \boldsymbol{\Psi}_2^{n-k+1} \ddot{\boldsymbol{u}}_{2,k} \tag{14}$$

where $\boldsymbol{\Psi}_2^k = \boldsymbol{Z}_m^k \tilde{\boldsymbol{M}}_\Gamma$. The coefficients corresponding to $\boldsymbol{Z}_m^k$ can be efficiently computed by using Fast Fourier Transforms (FFT) [10]:

$$\boldsymbol{Z}_{\boldsymbol{m}}^{\boldsymbol{k}} = \frac{\rho^{-n}}{L} \sum_{l=0}^{L-1} \hat{\boldsymbol{Z}}_m(s_l) e^{-\frac{2\pi i n l}{L}},\ n = 0, 1, .., N \tag{15}$$

where ρ represents the radius of a circle in the analyticity domain of $\hat{\boldsymbol{Z}}_m(s) = s^{-2} \hat{\boldsymbol{Z}}(s) \tilde{\boldsymbol{M}}_\Gamma^{-1}$ and $s_l = \frac{\delta(\rho e^{2\pi i l/L})}{\Delta t}$ with $\delta(\zeta)$ the polynomial of the underlying linear multistep method. Assuming that the values of $\hat{\boldsymbol{Z}}_m$ are computed with precision ϵ_{CQM}, one gets that the error in $\boldsymbol{Z}_{\boldsymbol{m}}^{\boldsymbol{k}}$ is $O(\sqrt{\epsilon_{CQM}})$ when $L = N$ and $\rho^N = \sqrt{\epsilon_{CQM}}$. In addition, the FFT algorithm allows to compute the weights in $O(L \log L)$ operations.

The governing equations are finally solved for displacement by using the modified average acceleration time integration scheme of the Newmark family. This time integration scheme allows to introduce numerical damping by means of the parameter α. Two different yields of plasticity $\boldsymbol{F}_{y1}$ and $\boldsymbol{F}_{y2}$ with $\boldsymbol{F}_{y1} >> \boldsymbol{F}_{y2}$. For both cases, Equations 13 have been solved for different accuracies ϵ_{CQM}. In the following, normalized errors during the first T seconds of the earthquake are calculated using the expression $e_T = \frac{RMS(\boldsymbol{u}-\boldsymbol{u}_{ref})}{max(\boldsymbol{u}_{ref})}$ where RMS and $\boldsymbol{u}_{ref}$ denote respectively the Root Mean Square and the reference solution. Table 2 presents the errors $e_{10}(\%)$ on the displacement of m_1 in the x-direction. No numerical damping is introduced ($\alpha = 0$).

ϵ_{CQM}	$e_T(\%)$
10^{-04}	5.81
10^{-06}	0.76
10^{-08}	1.29
10^{-10}	1.51
10^{-12}	1.53

(a)

ϵ_{CQM}	$e_T(\%)$
10^{-04}	62.82
10^{-06}	2.59
10^{-08}	2.73
10^{-10}	3.29
10^{-12}	3.34

(b)

Table 2: Relative errors for different precisions ϵ_{CQM} when the displacement at the top of the structure is computed during $T = 10s$ for (a) $\boldsymbol{F}_{y1}$ and (b) $\boldsymbol{F}_{y2}$, with $\boldsymbol{F}_{y1} >> \boldsymbol{F}_{y2}$ and $\alpha = 0$.

Results presented in Tables 2 show that better agreements with the reference solution are obtained for a precision of $\epsilon_{CQM} = 10^{-06}$ with both yields of plasticity. In addition, it seems that the more nonlinear the response, the larger the error. In fact, if numerical damping is introduced ($\alpha = 0.1$) for the reference solution computed with $\boldsymbol{F}_{y2}$ and $\epsilon_{CQM} = 10^{-06}$, the measured relative error reduces to $e_{10} = 1.59\%$. The observed dissipation is less important for $\boldsymbol{F}_{y1}$. Therefore, the numerical damping introduced by the proposed approach may come from the Newton nonlinear solver.

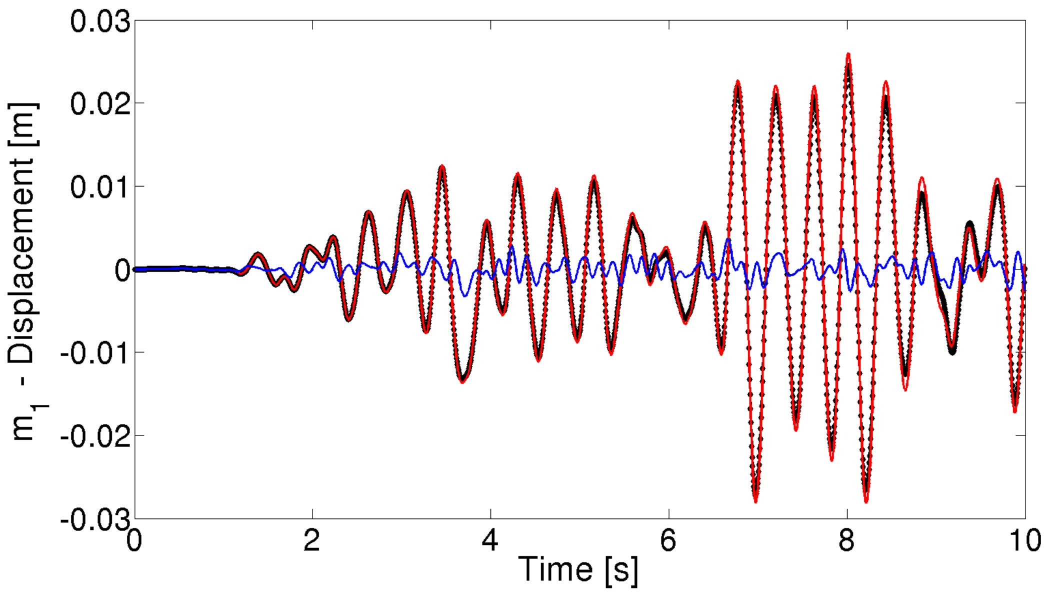

Figure 3: Displacement at m_1 in the x-direction computed with the hybrid time-Laplace domain approach (black markers) and compared to the reference solution (red line) and to the linear response (blue line) for $\boldsymbol{F}_{y2}$.

It should be remarked that if the plasticity yield is chosen sufficiently large, the entire calculation remains linear. Therefore, linear and nonlinear responses can easily be compared using a fixed precision, for example $\epsilon = 10^{-06}$. Figure 3 shows thus the displacement at m_1 in the x-direction compared to the reference solution and also to the linear solution for $\boldsymbol{F}_{y2}$. It is then observed that the amplitude of displacements is increased as expected. In addition, when the elastoplastic effects are taken into account, the structural response is clearly shifted to the low frequencies because of the reduction in stiffness ($\boldsymbol{K}_{e,i} > \boldsymbol{K}_{p,i}$). However, only one fundamental frequency seems to stand out in the response as if just one equivalent stiffness were present in the system. Hence, the effects of both stiffness $\boldsymbol{K}_e$ and $\boldsymbol{K}_p$ on the response can be highlighted by increasing the yield of plasticity. The response with a larger $\boldsymbol{F}_y$, plotted in Figure 4, is significantly different from the one plotted in Figure 3 showing in particular a higher frequency content.

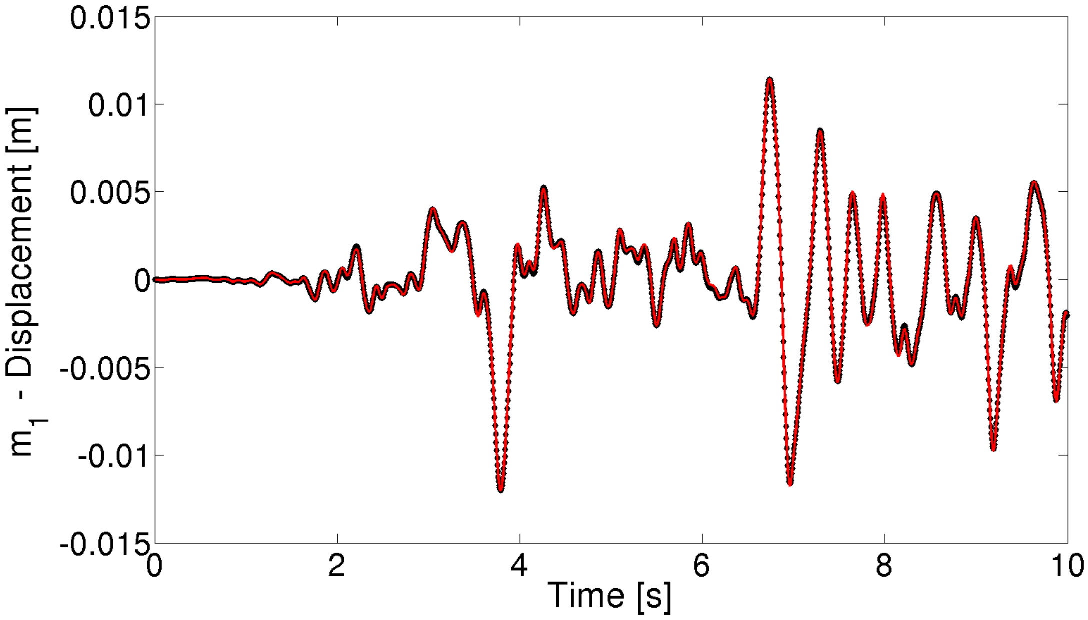

Figure 4: Displacement at m_1 in the x-direction computed with the hybrid time-Laplace domain approach (black markers) and compared to the reference solution (red line) for $\boldsymbol{F}_{y1}$.

Further research has to be pursued in order to investigate if the numerical response is improved when the damping and stiffness parts of the dynamic impedance are also factorized.

4 CONCLUSIONS

The soil-structure interaction problem is solved directly in the building and the impedance operator, defined on the boundary, is used as a particular type of boundary conditions that accounts for the unbounded soil. When nonlinearities are taken into account, the problem is solved in the time domain. Therefore, the influence of the soil is accounted for as a load (interaction forces) computed as a convolution integral in the time domain.

The proposed approach based on the Laplace domain presents some interesting features. On the one hand, it can be combined with IFFT algorithms yielding to small computational costs. On the other hand, it allows to express the convolution integral in terms of inertial, damping and stiffness quantities.

A numerical application considering nonlinear phenomena in the structure has been studied. The convolution integral has been transform to a convolution depending only on acceleration quantities. Very satisfactory results have been obtained when compared to a reference solution. However, it seems that the proposed approach introduces numerical damping when strong elastoplastic behaviour is taken into account.

REFERENCES

[1] G. R. Darbre and J. P. Wolf, Criterion of stability and implementation issues of hybrid frequency time domain procedure for non-linear dynamic analysis. *Earthquake Engineering and Structural Dynamics*, **16** (4), 569–581, 1988.

[2] J. P. Wolf, *Soil-Structure-Interaction Analysis in Time Domain*. Prentice-Hall, NJ, USA, 1988.

[3] R. Cottereau, D. Clouteau, C. Soize and S. Cambier, Probabilistic nonparametric models of impedance matrices. Application to the seismic design of a structure. *European Journal of Computational Mechanics*, **15**, 131–142, 2006.

[4] L. Gaul and M. Schanz, A comparative study of three boundary element approaches to calculate the transient response of viscoelastic solids with unbounded domains, *Computer Methods in Applied Mechanics and Engineering*, **179**, 111–123, 1999.

[5] M. Schanz and H. Antes, Aplication of 'Operational Quadrature Methods' in Time Domain Boundary Element Methods, *Meccanica*, **32** (3), 179–186, 2006.

[6] C. Lubich, Convolution quadrature and discretized operational calculus I. *Numerische Mathematik*, **52**, 129–145, 1988.

[7] W. Moser and H. Antes and G. Beer, A Duhamel integral based approach to one-dimensional wave propagation analysis in layered media, *Computational Mechanics*, **35**, 115–126, 2005.

[8] W. Moser and H. Antes and G. Beer, Soil-structure interaction and wave propagation problems in 2D by a Duhamel integral based approach and the convolution quadrature method, *Computational Mechanics*, **36**, 431–443, 2005.

[9] A. Pereira and G. Beer, Interface dynamic stiffness matrix approach for three-dimensional transient multi-region boundary element analysis. *International Journal for Numerical Methods in Engineering*, **80**, 1463–1495, 2009.

[10] C. Lubich, Convolution quadrature and discretized operational calculus II. *Numerische Mathematik*, **52**, 413–425, 1988.